Evolution of the Process for the Preparation of a Selective ErbB VEGF Receptor Inhibitor

Boguslaw Mudryk,* Amit Joshi,* Adrian Ortiz, Ian S. Young, James R. Sawyer, Bin Zheng, Masano Sugiyama, Zhongping Shi, Jale Müslehiddinoğlu,[1] R. Michael Corbett,[2] David R. Kronenthal, David A. Conlon

Chemical Development, Bristol-Myers Squibb Company, One Squibb Drive, New Brunswick, NJ 08903, USA
Fax +1(732)2273001; E-mail: boguslaw.mudryk@bms.com; E-mail: amit.joshi@bms.com

Received: 01.10.2012; Accepted: 17.10.2012

Abstract: An efficient synthetic route to the potent and selective ErbB VEGF receptor inhibitor, BMS-690514 (**1**) is described. Strategic modifications in both approach and procedure addressed several issues, which led to a safe, efficient, and economical process for the preparation of multi-kilogram quantities of **1**. The convergent route involves alkylation of a suitably protected (3*R*,4*R*)-4-aminopiperidin-3-ol with the triethyl(alkyl)ammonium salt of a functionalized pyrrolotriazine **3a** followed by deprotection to provide **1** as the crystalline free base.

Key words: antitumor agents, protected piperidines, protecting groups, heterocycles, Schiff bases

The human epidermal growth factor receptor (HER or EGFR) and the vascular endothelial growth factor receptor (VEGFR) signaling pathways are implicated in processes governing tumor growth and proliferation. The development of potent and selective inhibitors of HER and VEGFR may provide additional clinical benefit in the treatment of non-small-cell lung cancer (NSCLC), metastatic breast cancer, and other solid malignancies. As part of a drug discovery program at Bristol-Myers Squibb, the functionalized pyrrolotriazine BMS-690514 (**1**) was identified as an orally active, selective, and potent dual inhibitor of both HER and VEGFR.[3,4]

Herein, we report the process development and demonstration on multi-kilogram scale of a synthetic route to **1** that supports preclinical and clinical studies. In addition, we describe our laboratory development efforts towards an optimized end game, resulting in a process that should be viable on a commercial scale.

The retrosynthetic analysis of **1** is outlined in Scheme 1. Strategic C–N bond scission simplifies the target molecule into its constituent parts: enantiomerically pure piperidine **2** and pyrrolotriazine **3a**. In the forward sense, these fragments could be united by activation of the primary alcohol of **3a**, and alkylation with variably protected piperidine **2**. To ensure the success of this key step, we anticipated that a judicious selection of protecting groups would be required for the C-4 amino group present in **2** (see below). Finally, removal of the protecting groups would provide the target structure **1** as the crystalline free base.

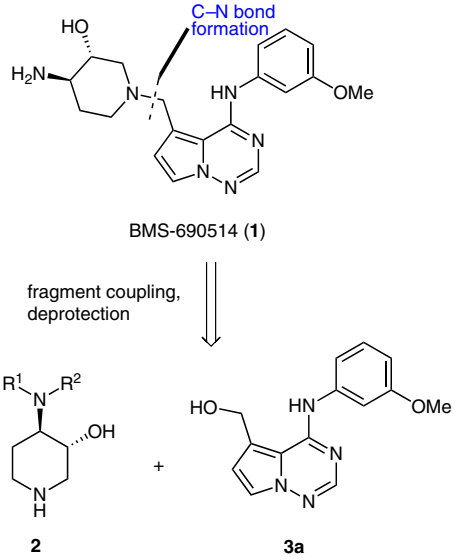

Scheme 1 Retrosynthetic analysis of BMS-690514 (**1**)

To support non-clinical and clinical studies, multi-kilogram quantities of both pyrrolotriazine **3a** and piperidine **2** were required. A scalable and efficient route to functionalized pyrrolotriazine **3a** was developed and is summarized retrosynthetically in Scheme 2. This work has been described in detail in a previous report.[5]

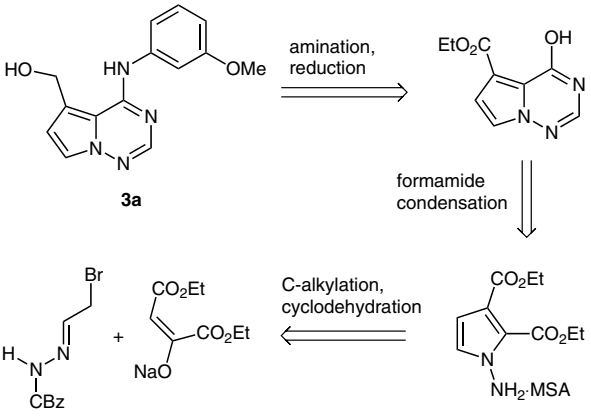

Scheme 2 Retrosynthetic analysis of pyrrolotriazine core **3a**

In 1998, Langlois and Calvez reported the synthesis of (3*S*,4*S*)-l-benzyl-4-*N*-benzylamino-3-hydroxypiperidine [(+)-**4a**] through ring expansion of (2*S*,3*S*)-l-benzyl-3-*N*-

SYNLETT 2013, 24, 0305–0312
Advanced online publication: 23.11.2012
DOI: 10.1055/s-0032-1317540; Art ID: ST-2012-Y0838-C

benzylamino-2-hydroxymethylpyrrolidine,[6] which was derived from (*S*)-pyroglutamic acid.[7] Our original route (see Scheme 3) to the enantiomer [(–)-**4a**] utilized a similar synthetic sequence with sequential Boc protection and selective debenzylation as the last two steps to arrive at intermediate **2a** (R^1 = Boc, R^2 = H).[4h] This sequence required some procedural modifications to enable the safe, efficient, and reproducible preparation of piperidine **4a** on scale (see the Supporting Information for more details). Ultimately, the seven-step process proceeded in 22% overall yield, and was successfully scaled to 70 kg without major issues. The final two transformations (**4a** → **2a**; Boc protection, followed by selective debenzylation) were telescoped to provide high quality **2a** after crystallization. With the orthogonally protected piperidine **2a** and pyrrolotriazine **3a** in hand, we turned our attention to the remaining transformations of the process, as shown in Scheme 4.

To this end, the fragment coupling of **3a** with the piperidine **2a** required activation of the primary alcohol. Initial attempts to prepare and directly couple the mesylate of **3a** resulted in an unsatisfactory impurity profile. Our colleagues in Discovery Chemistry had previously shown that the corresponding bromide reacted with triethylamine to produce the triethyl(alkyl)ammonium bromide, which could then be used to N-alkylate multiple piperidine derivatives in good yields.[4h] After surveying other reagents for activation of the alcohol, we found that the tetraalkylammonium derivative **3b** was formed most efficiently by displacement of the mesylate by triethylamine. Derivative **3b** was then coupled efficiently with **2a** to produce **5** in excellent yield and purity. Interestingly, replacing triethylamine with diisopropylethylamine did not lead to formation of the desired tetralkylammonium salt, presumably for steric reasons.

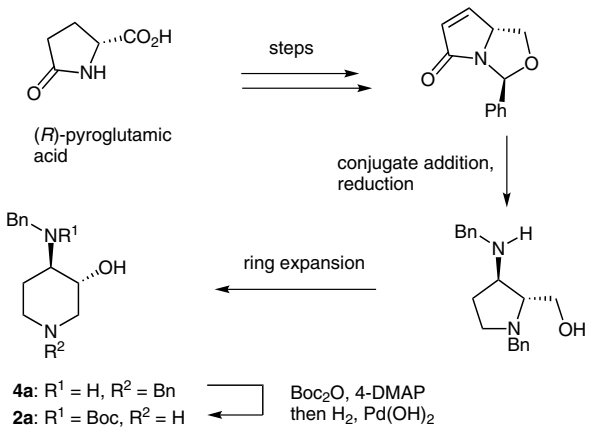

Scheme 3 Summary of the original synthetic route to fragment **2a**

One of the major impurities (**7**) from this step originated from an undesired Friedel–Crafts alkylation pathway (see Scheme 5). This impurity became a significant concern due to the poor downstream purging of subsequently formed derivatives. Upon identifying the triethyl(alkyl)ammonium salt as the preferred coupling partner, additional parameters (solvent, temperature, and stoichiometry) were studied to determine their impact on the level of the Friedel–Crafts impurity **7**. The key process parameter for control of the level of this impurity was found to be solvent, wherein *N*-methyl-2-pyrrolidinone (NMP) produced the lowest level of the impurity and was therefore selected for further development.[8]

The exothermic nature of both the mesylation and subsequent quaternization in NMP required these stages of the process to be performed at low temperature (–20 to 0 °C), which also helped control levels of impurity **7**. However, once **3b** was formed, coupling with **2a** required 8–10 h at 55 °C for the reaction to reach completion. Efforts to accelerate the coupling by increasing the temperature resulted in increased levels of **7**. We reasoned that the use of a

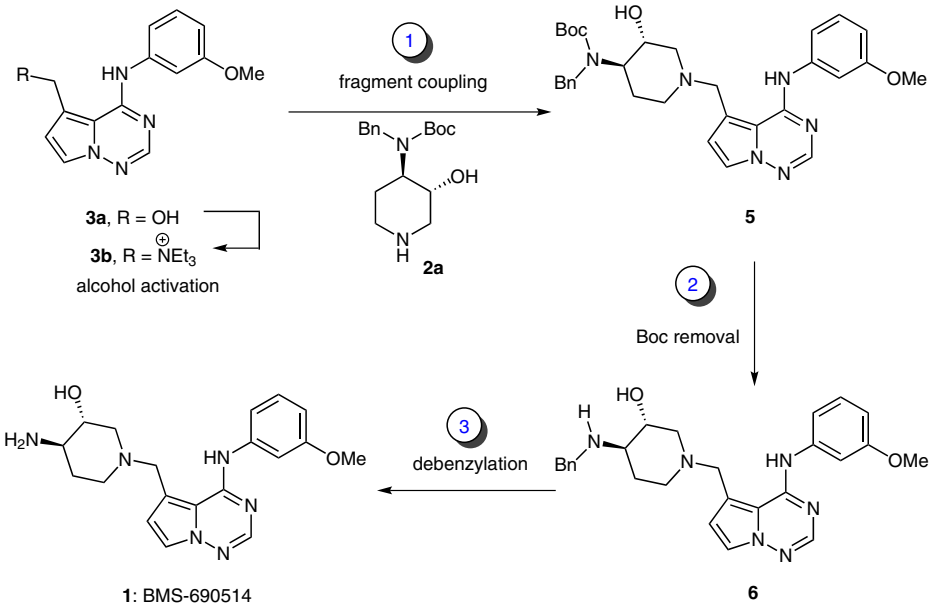

Scheme 4 Final steps to target structure **1**

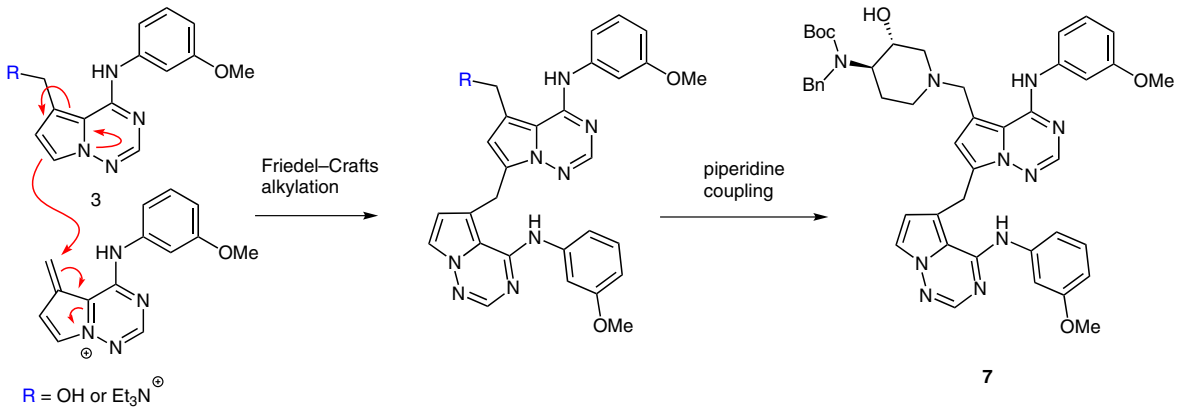

Scheme 5 Origin of the Friedel–Crafts impurity **7**

stronger base might accelerate the reaction. Indeed, the use of 1,8-diazabicyclo[5.4.0]undec-7-ene (DBU; 1–2 equiv) resulted in faster reactions (3 h at 55 °C); however, the yield was reduced by almost 5% due to the formation of a new impurity, **8**, arising from a competitive displacement process as illustrated in Scheme 6, therefore no additional studies were conducted with stronger bases.[9]

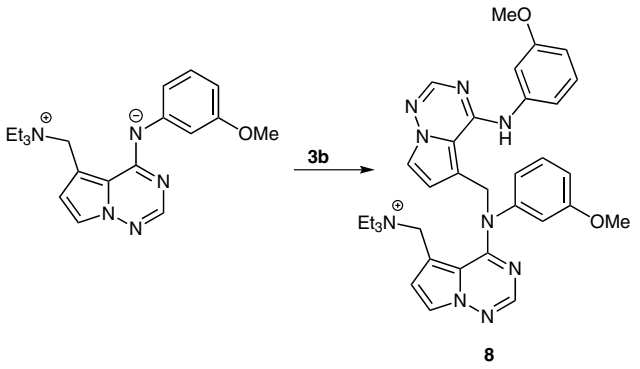

Scheme 6 Origin of the pseudodimeric impurity **8**

To ensure that our conversion and impurity specifications were achieved, we settled on the following optimized stoichiometry for this step: 3.9 equiv of triethylamine, 1.3 equiv of methanesulfonyl chloride and 1.1 equiv of **2a**. Combination of this stoichiometry and temperature range allowed consistent control of **7** to levels below 0.4 LCAP (liquid chromatography area percent). Addition of water to the process stream after reaction completion allowed direct precipitation of **5** and isolation by filtration. From a processing perspective, it was found that including an equivolume amount of acetonitrile as a cosolvent in the coupling step improved the crystallization of **5**, with minimal impact on the level of **7**. The finalized process, as shown in Scheme 7, was successfully scaled up to ca. 100 kg scale.

As the project advanced and additional material was required to support clinical trials, we reinvestigated the coupling process with the aim of improving it further. We observed that loss of acetonitrile and triethylamine during the coupling could lead to the reaction stalling, and increased impurity levels.[10] We also found that the presence of trace levels of oxygen during the coupling reaction led to highly colored reaction streams that resulted in an isolated product with a pink color. Recrystallization did not remove the colored impurities, which persisted in the downstream chemistry. We subsequently observed that the colored impurities were removed in the API (active pharmaceutical ingredient) debenzylation step, which used $Pd(OH)_2/C$ for hydrogenolysis, suggesting that use of activated carbon could result in color removal. An optional carbon treatment (Darco G60) was defined to remove color from the reaction stream during the formation of **6** (see below) if necessary.[11]

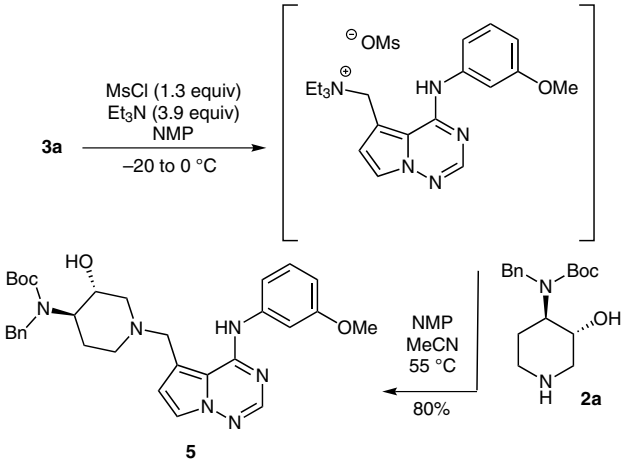

Scheme 7 Antepenultimate step: alkylation of piperidine **2a** and pyrrolotriazine **3a**

Additional effort was invested in making the crystallization of **5** more robust. Although the original crystallization of **5** (addition of water to the reaction stream at 25 °C) was simple to perform, it was inconsistent with regards to several key parameters. In particular, the time required for the crystallization to initiate varied, and in some instances the product oiled out of solution. Addition of 1 wt% of **5** seed at 40 °C prior to water addition, and slow cooling of the slurry to 25 °C over 2 h, resulted in a more consistent crystallization. In addition, the new procedure offered the advantage of an additional 40% purging of the Friedel–

Crafts pseudodimer impurity **7**. Two batches (ca. 30 kg) were executed in our pilot plant, with an average yield of 76%, to afford the isolated product with a purity of 99.4 LCAP and 100% ee, and an acceptable level of **7** (0.3 LCAP).

The penultimate step (Scheme 8) consists of acid-mediated Boc deprotection of **5** to provide **6** as a salt. Carbon dioxide and isobutylene are byproducts of this reaction. For safety reasons, the acid was added slowly at 50 °C to control the rate of CO_2 off-gassing. Most of the isobutylene remains in solution and is trapped by water to form *t*-BuOH. The penultimate salt is then free based by slow addition of 1 M NaOH, which affords crystalline **6**.

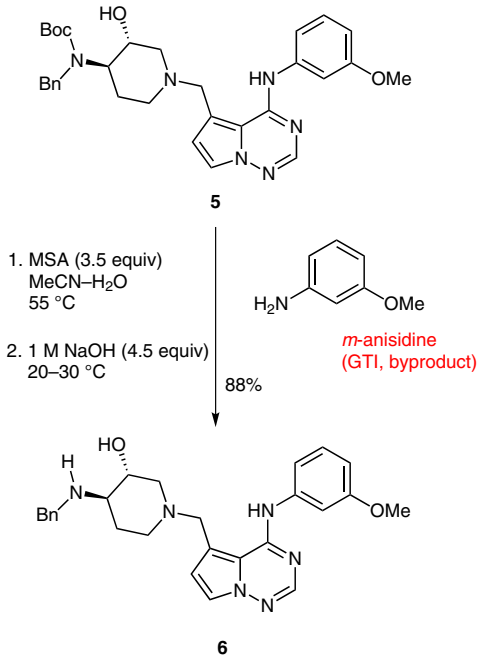

Scheme 8 Penultimate step: Boc deprotection of intermediate **5**

In the first process iteration, aqueous hydrochloric acid in isopropanol was used for the deprotection. Although Boc removal appeared simple from a chemistry perspective, it was complicated by the fact that *m*-anisidine was liberated as a byproduct of acidic hydrolysis of **5** and **6** (Scheme 8). *m*-Anisidine has been identified as a genotoxic impurity (GTI), therefore the level of this compound in the final isolated API needed to be controlled to below 5 ppm.[12] The observed level of *m*-anisidine in the reaction mixture was 700–1600 ppm, with up to 250 ppm present in isolated **6**. Based on the ability of the API crystallization to purge *m*-anisidine, a specification of <250 ppm of *m*-anisidine in isolated **6** was set.

As an alternative to HCl, we found that methanesulfonic acid in acetonitrile produced lower levels of *m*-anisidine in-process (200–400 ppm vs. 700–1600 ppm with HCl/IPA) and had the added advantage of slightly higher isolated yields (95 vs. 92%). The modified process consistently generated **6** with less than 100 ppm *m*-anisidine in the isolated solid, which was further reduced to acceptable levels in the API crystallization.

Three low-level impurities were observed in isolated **6**. Compound **9** (Figure 1) resulted from deprotection of the Friedel–Crafts impurity **7**, which was carried into the reaction with input **5**. Only modest reduction (ca. 40%) of this impurity was observed during the isolation of **6**, further confirming the necessity of controlling its formation in the preparation of **5**. The *tert*-butyl ether impurity **10** originated from reaction of the *tert*-butyl cation, formed during Boc removal, with the product.[13] Although **10** did not purge appreciably, its level was low enough (typically less than 0.2 LCAP) to not pose quality issues downstream. The final impurity of note in isolated **6** was the starting material **5**.

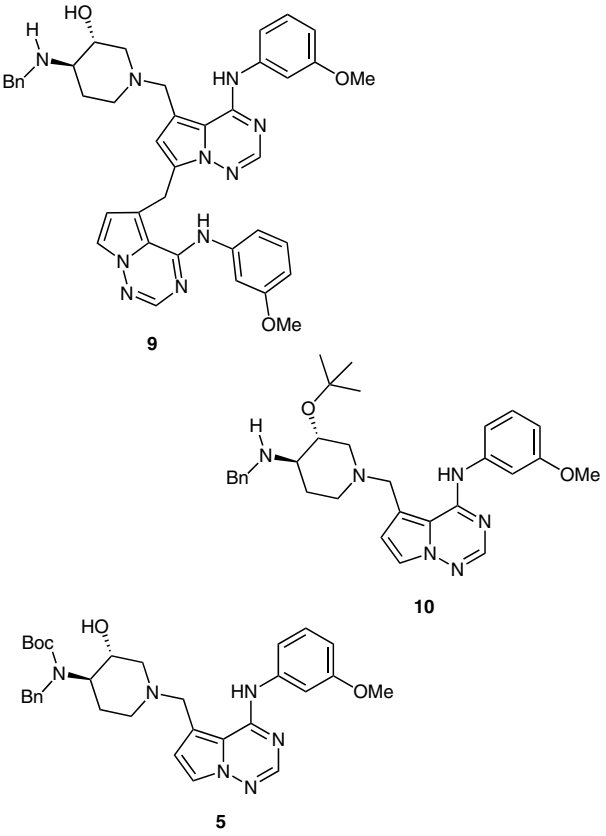

Figure 1 Key impurities for the penultimate step

Due to concerns with respect to *m*-anisidine formation, the reaction was closely monitored and not allowed to proceed past 98% conversion. As a result, some residual **5** (<2 LCAP) remained in the isolated product, which was acceptable since **5** was readily purged in the API step. We also monitored the process for acetamide (a potential carcinogen) due to the use of aqueous acid in acetonitrile at elevated temperatures. Analysis of the reaction stream revealed that acetamide was present at low levels (ca. 35 ppm), but was purged to undetectable levels in the isolated solid. This process was run at ca. 50 kg scale (two batches) to produce **6** in 94% yield with an average purity of 98.5 LCAP.

The final step (see Scheme 9) involved removal of the benzyl group by hydrogenolysis [20% $Pd(OH)_2/C$, 30 psig H_2, isobutanol/toluene, sodium carbonate,[14] 50 °C]. Upon completion of the reaction and filtration of the catalyst, the crude stream was washed with water and solvent exchanged to toluene, which facilitated the direct crystallization of **1**. The key to success of the hydrogenolysis was the judicious choice of solvent. Factors considered included: (1) solubility of the input and product; (2) product loss during the work-up; (3) degree of palladium leaching; (4) reaction kinetics; (5) impurity profile, and (6) robustness of the crystallization to ensure the correct API polymorph. Alcohol solvents or tetrahydrofuran (THF) were required to solubilize **6**, however, these solvents led to palladium leaching and unacceptable palladium levels in the final product. The addition of toluene as a cosolvent reduced the amount of palladium leaching and, importantly, led to the correct polymorph of the API during crystallization. A mixture of isobutanol/toluene (1:4 ratio) offered the advantage of near quantitative partitioning of the product into the organic phase during the aqueous wash. In this solvent system, Pearlman's catalyst [20% $Pd(OH)_2/C$] was found to be optimal, based on reaction rate and impurity profile.

During the hydrogenolysis, three impurities of concern were generated (**11**–**13**; Scheme 9B) in addition to derivatives of the three impurities present in compound **6** (**9**, **10**, and **5**) that also underwent debenzylation in this step.[15] The *N*-alkyl impurities, **11** and **13**, were formed by reductive amination of formaldehyde and isobutyraldehyde, respectively, which were contaminants present in isobutanol. Additionally, isobutyraldehyde could form by dehydrogenation (oxidation) of isobutanol mediated by the Pd catalyst. The *N*-methyl impurity **11** purged only 50% during the crystallization and posed the greatest liability. To ensure that acceptable levels of **11** were observed in the API, based on our purging studies, we set a specification of <100 ppm for formaldehyde in isobutanol. The *N*-isobutyl impurity **13**, however, purged efficiently in the crystallization and was not a concern. The *N*-ethyl impurity **12** was derived from reaction of the product with residual acetonitrile carried over from the previous step[16] and purged to >75% during the crystallization. To control the formation of **12**, we ensured that the level of acetonitrile present in **6** was less than 0.7%.[17] Isolation of **1** consisted of a water wash to remove the sodium carbonate, solvent swap to toluene by constant volume distillation (to less than 1% isobutanol), seeding (3 wt%, at 85–89 °C), and then slow cooling to 20 °C. This protocol reduced the levels of all the impurities (**11**–**13**) generated in the hydrogenolysis to acceptable levels. The crystallization also effectively purged *m*-anisidine from as high as 800 ppm to below 5 ppm.[18] Whereas the crystallization offered minimal reduction in the level of the debenzylated version of the Friedel–Crafts-derived impurity **9**, optimization of the coupling step (**3a** → **5**) allowed it to be controlled to acceptable levels upstream. This process yielded **1** (89% yield, potency of 99.3 wt%) on ca. 30 kg scale as a white solid, and consistently produced the correct crystal form of the API.

Despite the success and robustness of our initial deprotection endgame sequence, opportunities for improvement were identified in the following areas: (1) Boc deprotection (penultimate step) resulted in the liberation of the genotoxic impurity *m*-anisidine, and (2) benzyl group hydrogenolysis (API step) produced three potentially difficult to purge *N*-alkyl impurities. Due to these liabilities it became evident that an alternative endgame strategy

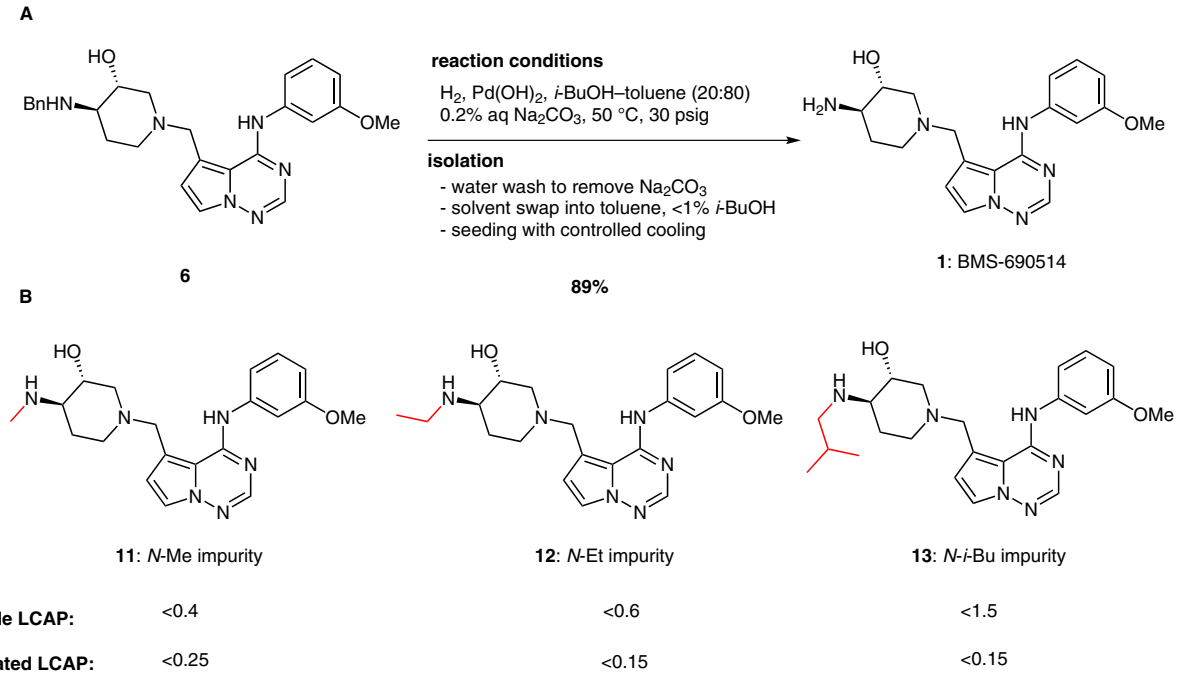

Scheme 9 (A) Hydrogenolysis of intermediate **6**; (B) key impurities (**11**–**13**) derived from hydrogenolysis of **6**

would need to be identified. In addition, whereas the process utilized to generate piperidine **2a** performed well on a multi-kilogram scale (see Scheme 3), it was laborious and operationally intensive because each transformation required multi-operation steps, decreased throughput and resulted in higher manufacturing costs (longer plant time).

All of the above considerations resulted in the development of a second-generation, more efficient synthesis of the target structure **1**. We first sought to develop an alternative preparation of piperidine **4a**. This study has been recently reported[19] and is summarized retrosynthetically in Scheme 10. This alternative chemistry resulted in the development of an expedient and simple racemic synthesis of **4a** from pyridine and benzyl chloride followed by a classical resolution.

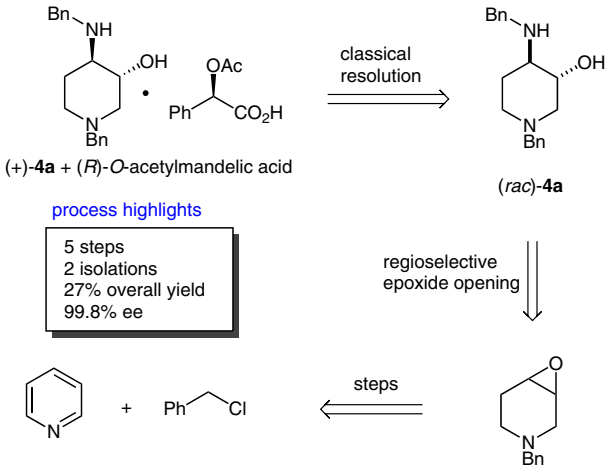

Scheme 10 Second generation synthesis of **4a**

Secondly, it was quickly recognized that these end game liabilities / impurities were a consequence of protecting group choice, and therefore could conceivably be avoided by simply adjusting the protecting group strategy without changing the overall synthetic strategy. As an alternative, a Schiff base strategy was envisaged (Scheme 11) to replace the initial Boc/Bn strategy (Scheme 7).

Upon initial evaluation of this alternative protection strategy, there were concerns that the perceived instability of Schiff bases might render this approach impractical. A survey of the literature provided a recent example that utilized methyl isobutyl ketone (reaction solvent) to mask a primary amine in situ as the Schiff base. This allowed selective alkylation of a secondary amine present within the molecule.[20] Further precedence was garnered from the demonstration that (1*R*,2*R*)-2-aminocyclohexanol produces stable Schiff bases with benzaldehyde, in contrast to the (1*R*,2*S*)-2-aminocyclohexanol, which yields the oxazolidine (Scheme 12).[21] With this knowledge providing a degree of confidence, the first task at hand was selection of the appropriate aldehyde component. We imposed three selection criteria: (1) the aldehyde must be inexpensive, (2) the resultant Schiff base intermediates must be isolable crystalline solids, and (3) these isolated solids must possess sufficient stability to enable isolation and prolonged storage. After screening a series of aldehydes, we found that *p*-anisaldehyde satisfied all these requirements.

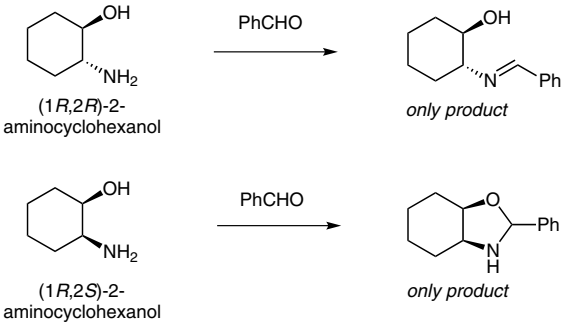

Scheme 12 Precedence for stable Schiff base vs. oxazolidine formation

This alternative sequence was successfully demonstrated on a 300 g scale. Both benzyl groups present in **4a** were removed under hydrogenolysis conditions (H_2; 30 psig, Pd/C). The resulting crude ethanolic stream of **14** was then treated with *p*-anisaldehyde and the ethanol was ex-

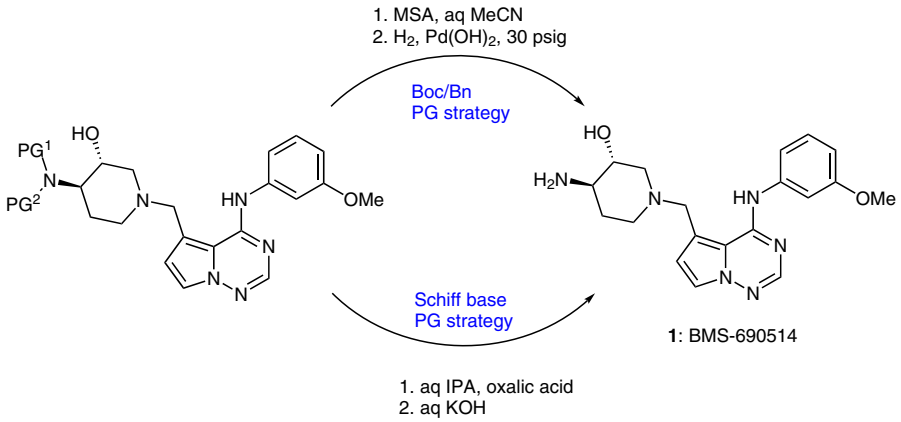

Scheme 11 Comparison of protecting group strategies

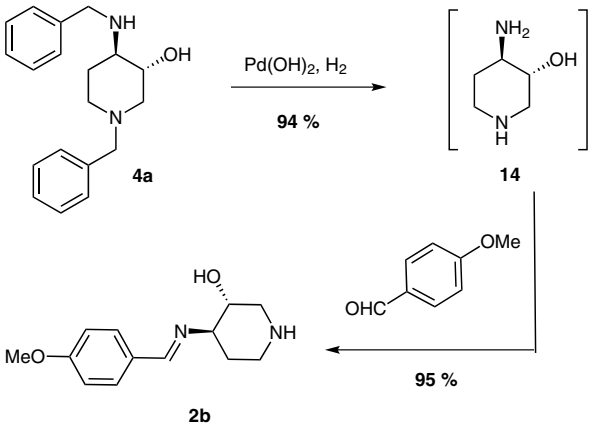

Scheme 13 Preparation of Schiff base **2b**

changed with toluene. During this process, the reaction was azeotropically driven to completion by removal of water, with concurrent crystallization of the desired product from the reaction mixture. Schiff base intermediate **2b** was isolated in 95% yield over these two steps (Scheme 13).

Subsequent coupling was performed as previously described (Scheme 14), however, in this case, NMP was used as the sole solvent rather than as a cosolvent with acetonitrile. Omission of acetonitrile allowed for a direct crystallization of the product through the addition of water upon reaction completion. This process resulted in a 76% yield of the isolated Schiff base **15** as its monohydrate. The level of the equivalent Schiff base pseudodimer was similar to the level of **7** produced under the original coupling conditions. Hydrolytic deprotection of the Schiff base was conducted under mild conditions (4% aq IPA, 1.5 equiv oxalic acid) and resulted in the isolation of **1** as the oxalate salt (97% yield). It is important to point out that a simple and mild acid hydrolysis has replaced two problematic steps, Boc removal and hydrogenolysis. Finally, conversion of the API into the desired polymorph required removal of oxalic acid (aq KOH) followed by crystallization from toluene (91% from **15**) as previously described. This process provided high quality API (Scheme 14) of the desired crystal form.[22]

A robust synthesis of **1**, which is a potential therapeutic agent for the treatment of lung and other cancers, has been described. The original route was used to prepare >100 kg of **1**, but suffered shortcomings that would hinder larger future deliveries. The use of a Schiff base for primary nitrogen protection during coupling of the two key fragments (**3**+**2**), alleviated many of the issues encountered with the previously used Boc/benzyl protecting groups (*m*-anisidine liberation during Boc removal and *N*-alkyl impurities generated during hydrogenolysis). This improved end game strategy was successfully demonstrated and produced 232 g of API of similar quality to the product obtained through the previous route. In addition to the technical advantages garnered by use of the Schiff base strategy, the yield was also improved for this new process (67 vs. 62%).

Acknowledgment

We would like to thank Drs. Robert Waltermire and Jean Tom for careful review of this manuscript. We also acknowledge the analytical support provided by Drs. Su Pan, Vera Leshchinskaya, Lydia Breckenridge, Charles Pathirana and Mr. Jonathan Karten. We thank our colleagues in Chemical Development Operations for their contributions to the development of these processes. We would also like to thank Dr. Yeung Chan, Dr. Daniel Hsieh, Dr. Simon Leung, Shawn Springfield, Agnes Yeboah, and Melissa Chau for their contributions to this work.

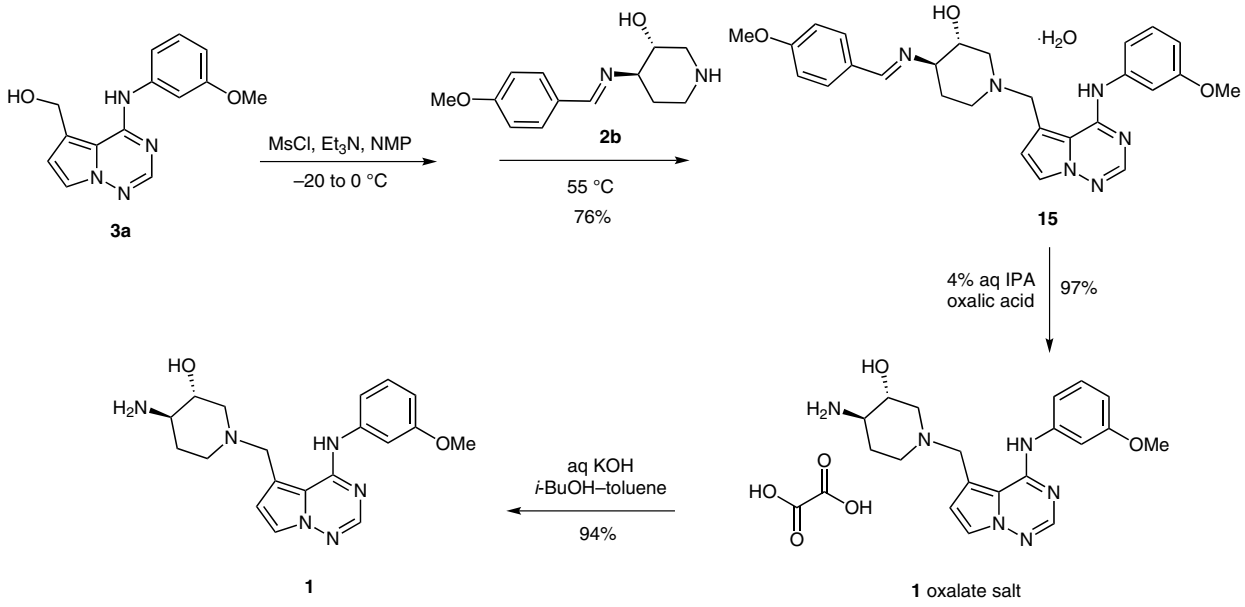

Scheme 14 Alternative end game strategy

Supporting Information for this article is available online at http://www.thieme-connect.com/ejournals/toc/synlett.

References and Notes

(1) New address: Celgene Corp., Basking Ridge, NJ, USA.
(2) New address: Dupont, Newark, DE, USA.
(3) For Bristol-Myers Squibb patents covering **1**, see: (a) Wei, C.; Norris, D. J. *Crystalline forms of (3R,4R)-4-amino-1-({4-[(3-methoxyphenyl)amino]pyrrolo[2,1-f][1,2,4]triazin-5-yl}methyl)piperidine-3-ol;* US Patent 0191375, **2007**. (b) Fink, B. E.; Gavai, A. V.; Vite, G. D.; Chen, P.; Mastalerz, H.; Norris, D. J.; Tokarshi, J. S.; Zhao, Y.; Han, W.-C. *Preparation of pyrrolo[2,1-f][1,2,4]triazine derivatives as HER1, HER2, HER4 kinase inhibitors and antiproliferative agents;* WO Patent 066176, **2005**. (c) Fink, B. E.; Gavai, A. V.; Vite, G. D.; Chen, P.; Mastalerz, H.; Norris, D. J.; Tokarski, J. S.; Zhao, Y.; Han, W.-C. *Pyrrolotriazine Compounds as Kinase Inhibitors;* US Patent 7,141,571 B2, **2006**.
(4) For earlier discovery work in the HER and VEGFR program, see: (a) Borzilleri, R. M.; Cai, Z.; Ellis, C.; Fargnoli, J.; Fura, A.; Gerhardt, B.; Goyal, B.; Hunt, J. T.; Mortillo, S.; Qian, L.; Tokarski, J.; Vyas, V.; Barri Wautlet, B.; Zhenga, X.; Bhidea, R. S. *Bioorg. Med. Chem. Lett.* **2005**, *15*, 1429. (b) Fink, B. E.; Vite, G. D.; Mastalerz, H.; Kadow, J. H.; Kim, S.-H.; Leavitt, K. J.; Du, K.; Crews, D.; Mitt, T.; Wong, T. W.; Hunt, J. T.; Vyas, D. M.; Tokarski, J. S. *Bioorg. Med. Chem. Lett.* **2005**, *17*, 4774. (c) Mastalerz, H.; Chang, M.; Chen, P.; Dextraze, P.; Fink, B. E.; Gavai, A.; Goyal, B.; Han, W.-C.; Johnson, W.; Langley, D.; Lee, F. Y.; Marathe, P.; Mathur, A.; Oppenheimer, S.; Ruediger, E.; Tarrant, J.; Tokarski, J. S.; Vite, G. D.; Vyas, D. M.; Wong, H.; Wong, T. W.; Zhang, H.; Zhang, G. *Bioorg. Med. Chem. Lett.* **2007**, *17*, 2036. (d) Mastalerz, H.; Chang, M.; Gavai, A.; Johnson, W.; Langley, D.; Lee, F. Y.; Marathe, P.; Mathur, A.; Oppenheimer, S.; Tarrant, J.; Tokarski, J. S.; Vite, G. D.; Vyas, D. M.; Wong, H.; Wong, T. W.; Zhang, H.; Zhang, G. *Bioorg. Med. Chem. Lett.* **2007**, *17*, 2828. (e) Mastalerz, H.; Chang, M.; Chen, P.; Fink, B. E.; Gavai, A.; Han, W.-C.; Johnson, W.; Langley, D.; Lee, F. Y.; Leavitt, K.; Marathe, P.; Norris, D.; Oppenheimer, S.; Sleczka, B.; Tarrant, J.; Tokarski, J. S.; Vite, G. D.; Vyas, D. M.; Wong, H.; Wong, T. W.; Zhang, H.; Zhang, G. *Bioorg. Med. Chem. Lett.* **2007**, *17*, 4947. (f) Cai, Z.-W.; Wei, D.; Borzilleri, R. M.; Qian, L.; Kamath, A.; Mortillo, S.; Wautlet, B.; Henley, B. J.; Jeyaseelan, R.; Tokarski, J.; Hunt, J. T.; Bhide, R. S.; Fargnoli, J.; Lombardo, L. J. *Bioorg. Med. Chem. Lett.* **2008**, *18*, 1354. (g) Gavai, A. V.; Fink, B. E.; Fairfax, D. J.; Martin, G. S.; Rossiter, L. M.; Holst, C. L.; Kim, S.-H.; Leavitt, K. J.; Mastalerz, H.; Han, W.-C.; Norris, D.; Goyal, B.; Swaminathan, S.; Patel, B.; Mathur, A.; Vyas, D. M.; Tokarski, J. S.; Yu, C.; Oppenheimer, S.; Zhang, H.; Marathe, P.; Fargnoli, J.; Lee, F. Y.; Wong, T. W.; Vite, G. D. *J. Med. Chem.* **2009**, *52*, 6527. (h) Fink, B. E.; Norris, D.; Mastalerz, H.; Chen, P.; Goyal, B.; Zhao, Y.; Kim, S.-H.; Vite, G. D.; Lee, F. Y.; Zhang, H.; Oppenheimer, S.; Tokarski, J. S.; Wong, T. W.; Gavai, A. V. *Bioorg. Med. Chem. Lett.* **2011**, *21*, 781.
(5) Zheng, B.; Conlon, D. A.; Corbett, R. M.; Chau, M.; Hsieh , D.-M.; Yeboah, A.; Hsieh, D.; Müslehiddinoğlu, J.; Gallagher, W. P.; Simon, J.-N.; Burt, J. *Org. Process Res. Dev.* **2012**, *16*, 1846.
(6) (a) Langlois, N.; Calvez, O. *Synth. Commun.* **1998**, *28*, 4471. (b) For other examples of this type of ring expansion see: Cossy, J.; Dumas, C.; Michel, P.; Pardo, G. M. *Tetrahedron Lett.* **1995**, *36*, 549. (c) See also: Cossy, J.; Dumas, C.; Pardo, G. M. *Synlett* **1997**, 905.
(7) Thottathil, J. K.; Moniot, J. L.; Mueller, R. H.; Wong, M. K. Y.; Kissick, T. P. *J. Org. Chem.* **1986**, *51*, 3140.
(8) Use of NMP produced approximately 1 LCAP of the Friedel–Crafts-derived impurity. As a comparison, CH_2Cl_2, which was the worst performer, produced ca. 12 LCAP of the impurity.
(9) The structure of **8** was proposed based on LCMS data. Specifically, the C–N connectivity cannot be confirmed.
(10) Loss of acetonitrile and triethylamine, which form a low-boiling azeotrope (b.p. 55 °C), was attributed to the nitrogen sweep used to ensure efficient inertion and prevent formation of colored impurities. This issue was resolved during development runs by using a nitrogen blanket, and was not observed in the pilot plant batches.
(11) Carbon treatment after formation of **5** resulted in ca. 5% Boc deprotection even at r.t. and, as a result, the carbon treatment should be implemented during processing of **6** if required.
(12) For a discussion on genotoxic impurities, see: Snodin, G. *J. Regul. Toxicol. Pharmacol.* **2006**, *45*, 79.
(13) The linkage of the *tert*-butyl group to oxygen was confirmed by HMBC NMR experiments.
(14) The aqueous carbonate was used in the first iteration of the process to neutralize hydrogen bromide, a byproduct derived from des-bromination of the brominated penultimate derivative at the pyrrole fragment; see ref. 4. Although the carbonate was not needed, it was retained in the revised process to accommodate regulatory requirements and keep the key process parameters unchanged.
(15) In general, impurities (organic, residual solvents, or inorganic) do not add any therapeutic value, may present toxicity concerns and are therefore controlled to very low levels in the active pharmaceutical ingredient.
(16) Nacario, R.; Kotakonda, S.; Fouchard, D. M. D.; Tillekeratne, L. M. V.; Hudson, R. A. *Org. Lett.* **2005**, *7*, 471.
(17) From a procedural perspective, it was noted that this impurity continued to form after the reaction reached its endpoint. As a result, we utilized an internal Raman probe, rather than HPLC after a set amount of time. This allowed us to stop the reaction when it was complete, minimizing additional conversion of **1** into **12.**
(18) It should be noted that we set a more stringent requirement of 250 ppm *m*-anisidine in isolated **6** (see above) to ensure that safe levels of this impurity would be present in the drug substance.
(19) (a) Young, I. S.; Ortiz, A.; Sawyer, J. R.; Conlon, D. A.; Buono, F. G.; Leung, S. W.; Burt, J. L.; Sortore, E. *Org. Process Res. Dev.* **2012**, *16*, 1558. (b) Ortiz, A.; Young, I. S.; Sawyer, J. R.; Hsiao, Y.; Singh, A.; Sugiyama, M.; Corbett, R. M.; Chau, M.; Shi, Z.; Conlon, D. A. *Org. Biomol. Chem.* **2012**, *10*, 5253. (c) First generation: 7 steps, 3 isolations, 26 operations, 22% overall yield. Second generation: 5 steps, 2 isolations, 10 operations, 29% overall yield resulting in 60% reduction in cost. Number of steps refers to number of intermediates that could be isolated.
(20) Laduron, F.; Tamborowski, V.; Moens, L.; Horváth, A.; De Smaele, D.; Leurs, S. *Org. Process Res. Dev.* **2005**, *9*, 102.
(21) Gil-Av, E. *J. Am. Chem. Soc.* **1959**, *81*, 1602.
(22) First generation: three steps, 62% yield, three *N*-alkyl impurities. Second generation: two steps, 67% yield, no *N*-alkyl impurities. Number of steps refers to number of intermediates that could be isolated.

